

# Some Supervision Required: Incorporating Oracle Policies in Reinforcement Learning via Epistemic Uncertainty Metrics

Jun Jet Tai,<sup>1</sup> JK Terry,<sup>2</sup> Mauro S. Innocente,<sup>3</sup> James Brusey,<sup>4</sup> Nadjim Horri,<sup>5</sup>

<sup>1 3 4 5</sup> Coventry University, UK

<sup>2</sup> University of Maryland, USA

<sup>1</sup> taij@uni.coventry.ac.uk, <sup>2</sup> jkterry@umd.edu, <sup>2</sup> mauro.s.innocente@coventry.ac.uk, <sup>4</sup> ab3853@coventry.ac.uk <sup>5</sup> aa3172@coventry.ac.uk

## Abstract

An inherent problem in reinforcement learning is coping with policies that are uncertain about what action to take (or the value of a state). Model uncertainty, more formally known as *epistemic uncertainty*, refers to the expected prediction error of a model beyond the sampling noise. In this paper, we propose a metric for epistemic uncertainty estimation in  $Q$ -value functions, which we term *pathwise epistemic uncertainty*. We further develop a method to compute its approximate upper bound, which we call  $F$ -value. We experimentally apply the latter to Deep Q-Networks (DQN) and show that uncertainty estimation in reinforcement learning serves as a useful indication of learning progress. We then propose a new approach to improving sample efficiency in actor-critic algorithms by learning from an existing (previously learned or hard-coded) oracle policy while uncertainty is high, aiming to avoid unproductive random actions during training. We term this *Critic Confidence Guided Exploration* (CCGE). We implement CCGE on Soft Actor-Critic (SAC) using our  $F$ -value metric, which we apply to a handful of popular Gym environments and show that it achieves better sample efficiency and total episodic reward than vanilla SAC in limited contexts.

## 1 Introduction

Reinforcement Learning (RL) seeks to learn a policy that maximizes the expected discounted future rewards for Markov Decision Process (MDP) (Sutton and Barto 2018). This contrasts to supervised learning, which seeks to learn a function to map data to labels. When presented with a dataset of states and actions from a given policy in an environment, a model can be trained using supervised learning to map the states to action in a way that mimics the dataset, which is called imitation learning (Bain and Sammut 1995; Liu et al. 2018; Ho, Gupta, and Ermon 2016).

In the actor critic framework for RL, an actor explores the environment enough for a critic to learn the reward structure of the environment. The actor then learns to take better actions by attempting to optimize the expected discounted future rewards as predicted by the critic. As such, the actor critic framework for RL can be viewed as a form of supervised learning (Eysenbach, Kumar, and Gupta 2020). Many of the most widely used methods in deep RL use the actor critic framework. For instance, they comprise four out of twelve algorithms in OpenAI Baselines (Dhariwal et al.

2017) and four out of seven algorithms in Stable-Baselines3 (Raffin et al. 2019).

To explore an environment during optimization, most popular methods generally employ stochastic actions to explore the environment (Lillicrap et al. 2016; Haarnoja et al. 2018b; Silver et al. 2014; Van Hasselt, Guez, and Silver 2016; Silver et al. 2016; Zhang, Pan, and Kochenderfer 2017; Schulman et al. 2017). As a result, at the beginning of training, a randomly initialized policy takes random actions as it has no understanding of the environment. In most environments, it is usually easy to create a simple policy that performs better than random via methods other than RL, e.g. hard-coding a policy to produce very basic behavior. We refer to this as an *oracle policy*. If an RL agent was able to learn from an oracle policy instead of trying random actions at the beginning of training, the number of samples required for its training could be reduced and/or its learning could be enhanced by improving the agent’s ability to escape local minima. This idea of bootstrapping from an oracle is hereafter referred to as *Critic Confidence Guided Exploration* (CCGE). In order to incorporate CCGE into an actor-critic algorithm, we theoretically derive and implement a method to estimate the uncertainty of the critic’s predictions and use that measure to control its influence during training. In other words, the oracle is favoured when uncertainty is high, with the critic gaining influence as the learning progresses.

This paper makes five contributions. First, we derive a quantity that we term *pathwise epistemic uncertainty*, which offers a formal metric of the epistemic uncertainty of the  $Q$ -value predictions during training (Section 4). Second, we derive a quantity that we term the  $F$ -value that is a learnable upperbound value to the pathwise epistemic uncertainty metric. Third, we propose a new strategy to improve sample efficiency via the use of oracle policies, which we term *Critic Confidence Guided Exploration* (CCGE) (Section 5.1). Fourth, we show a way to implement this metric in deep RL for Q-learning and for actor-critic based methods (Section 5.2). As expected, our metric is observed to provide insight into model learning, such as when an agent discovers a new high-reward state (Section 6.1). Fifth, we implement one form of CCGE using  $F$ -values and show that it can improve sample efficiency in PyBullet environments (Ellenberger 2018–2019) as well as reduce learning variance in a hyperparameter sensitive, domain-randomized Gym Car-

Racing environment (Brockman et al. 2016) (Section 6.2).

## 2 Related Work

### 2.1 Uncertainty in Reinforcement Learning

**The Intuition of Epistemic Uncertainty** When optimizing a model, knowing how much further performance could be improved given more training would be obviously helpful. In statistical learning theory, this general quantity is referred to as *Epistemic Uncertainty* (Matthies 2007), of which there are multiple formal quantifications. A naive approach is to use the variance of the model predictions as a proxy metric (Lakshminarayanan, Pritzel, and Blundell 2017; Gal and Ghahramani 2016), which does not distinguish between *aleatoric* and *epistemic* uncertainties. It is important to note that some authors like Lakshminarayanan, Pritzel, and Blundell (2017) and Gal and Ghahramani (2016) refer to the combined quantity as epistemic uncertainty. Conversely, evidential regression (Amini et al. 2020) separates these types of uncertainties by proposing evidential priors over the data likelihood function. However, this technique does not extend to nonstationary distributions, as is the case in policy conditioned  $Q$ -value predictions in RL. More recently, Jain et al. (2021) also attempted to model aleatoric and epistemic uncertainties by relating them to the expected prediction errors of the model. We postulate that this is a more epistemologically desirable way to measure epistemic uncertainty, as this relation directly predicts how much improvement can be gained given more data and learning capacity, whereas the evidential prior by Amini et al. (2020) is essentially a proxy metric.

**Prior Usage of Epistemic Uncertainty in Reinforcement Learning** Most of the previous uses of epistemic uncertainty in RL have revolved around using it to motivate exploration in more uncertain states (Moerland, Broekens, and Jonker 2017; Nikolov et al. 2018; Jain et al. 2021). It has also been used to build risk aware RL agents, which seek to maximize expected reward without venturing into an unfamiliar part of the environment during deployment (Osband 2016; Clements et al. 2019; Festor et al. 2021). These methods utilize the variance in predicted  $Q$ -values for single  $\{s_t, a_t\}$  pairs as a proxy to epistemic uncertainty, either via ensemble modelling or using distributional RL models. Additionally, Jain et al. (2021) perform epistemic uncertainty prediction on a limited case of exploration in RL by relating it to the single-step Bellman error.

### 2.2 Methods for Improving Sample Efficiency

There are several methods that aim to improve the sample efficiency of RL agents. Curriculum learning aims to accomplish this by forming a curriculum of different tasks that progressively become more difficult (Bengio et al. 2009) whilst model based RL aims to gain more detailed world knowledge of the environment more efficiently to reduce the number of steps that need to be taken in it (Hafner et al. 2019; Chen et al. 2022; Hafner et al. 2020; Schrittwieser et al. 2020). Other methods to improve the sample efficiency of RL are based on incorporating oracle policies, three of which are discussed next.

### Imitation Learning and Offline Reinforcement Learning

One method to improve sample efficiency of RL by leveraging oracle policies is to initialize training with policies obtained from imitation learning, as was famously done with AlphaGo using human experts as oracle policies (Silver et al. 2016). This can work reasonably well for policy gradient methods (Rajeswaran et al. 2018; Kober and Peters 2010), but can yield bad results when applied to actor-critic methods due to the critic not being well initialized on the policy (Zhang and Ma 2018; Nair et al. 2020). A similar line of work uses offline RL to initialize a learning policy by first training on prior data gathered by an oracle policy before interacting with the environment (Nair et al. 2018; Hester et al. 2018; Kumar et al. 2020; Sonabend et al. 2020). Another related method is to carry out environment rollouts by taking composite actions that are a weighted sum of the oracle’s actions and the learning policy’s actions (Rosenstein et al. 2004). As training progresses, the weighting is annealed to favour the learning policy’s actions over the oracle’s.

### Kullback-Leibler Regularized Reinforcement Learning

Kullback-Leibler (KL) regularized RL integrates an oracle policy by incorporating the oracle’s actions into the actor’s action distribution using an additional KL loss between the two distributions. This has been shown to work on actor critic methods on a range of RL benchmarks (Boularias, Kober, and Peters 2011; Nair et al. 2020; Ng, Russell et al. 2000; Peng et al. 2019; Siegel et al. 2019; Wu, Tucker, and Nachum 2019). However, in some cases, this can cause the actor to perform poorly when trying to assign probability mass to the singular action given by the oracle over a distribution of actions (Rudner et al. 2021).

### Jump-Start Reinforcement Learning

Uchendu et al. (2022) uses an oracle policy to step through the environment for a fixed number of steps, then switches to the learning policy to perform training thus effectively jump-starting RL training. The number of steps is gradually reduced as training progresses, forming a curriculum that can be gradually learned.

## 3 Background

### 3.1 Notation

This work uses the standard MDP definition and variables (Sutton and Barto 2018), with state  $s_t \in \mathbf{S}$ , action  $a_t \in \mathbf{A}$ , reward  $r_t(s_t, a_t, s_{t+1}) \in \mathbb{R}$  and environment state transition distribution  $\rho_{\text{env}}$ . During training, transition tuples of  $\{s_t, a_t, r_t, s_{t+1}\}$  are stored in a replay buffer  $\mathcal{D}$ , and the agent’s policy is  $\pi(a_t|s_t)$ .

### 3.2 Deep Q Network

The Deep Q Network (DQN) (Mnih et al. 2015) was one of the first deep RL algorithms, in which transition tuples are sampled from  $\mathcal{D}$  to learn a function  $Q^\pi : \mathbf{S} \times \mathbf{A} \rightarrow \mathbb{R}$  that minimizes the Bellman error by minimizing the loss function:

$$\mathcal{L}(s_t, a_t) = l(Q^\pi(s_t, a_t) - \mathbb{E}_\pi[r_t + \gamma Q^\pi(s_{t+1}, a_{t+1})]) \quad (1)$$

where  $l(\cdot)$  is usually the squared error loss (and is defined as so in the remainder of the paper) and  $\mathbb{E}_\pi$  denotes the expectation when acting according to the policy  $\pi$ . For DQN, the policy is defined as  $\pi(\mathbf{a}_t|\mathbf{s}_t) = \operatorname{argmax}_{\mathbf{a}_t} Q(\mathbf{s}_t, \mathbf{a}_t)$ . This loss function will be used in derivations later in this work.

### 3.3 Soft Actor Critic (SAC)

The Soft Actor Critic (SAC) algorithm is an entropy regularized actor critic algorithm introduced in (Haarnoja et al. 2018a). This work specifically refers to SAC-v2 (Haarnoja et al. 2018b) as SAC, a slightly improved variant with twin delayed Q networks and automatic entropy tuning. SAC has a pair of models parameterized by  $\theta$  and  $\phi$  that represent the actor  $\pi_\theta$  and the critic  $Q_\phi^\pi$ . The critic is a modified version of DQN with entropy regularization that works with continuous action spaces. The actor is optimized by minimizing the following loss function via the critic:

$$\mathcal{L}_\pi(Q_\phi^\pi, \pi_\theta) = -\mathbb{E}_{\substack{\mathbf{s}_t \sim \mathcal{D} \\ \mathbf{a}_t \sim \pi_\theta}} [Q_\phi^\pi(\mathbf{s}_t, \mathbf{a}_t)] \quad (2)$$

This loss function will be used in derivations later in this work. Note that we have dropped the long entropy term for brevity as it is not relevant to our derivations, but it can be viewed in the formulation by Haarnoja et al. (2018b).

### 3.4 Formalism of Epistemic Uncertainty

We present the formalism for epistemic uncertainty presented by Jain et al. (2021) and the related definitions in the notation that will be used in this paper. Consider a learned function  $f$  that tries to minimize the expected value of the loss  $l(f(x) - y)$  where  $y \sim P(\mathcal{Y}|x)$ .

**Definition 1** The *total uncertainty*  $\mathcal{U}(f, x)$  of a function  $f$  at an input  $x$ , is defined as the expected loss  $l(f(x) - y)$  under the conditional distribution  $y \sim P(\mathcal{Y}|x)$ .

$$\mathcal{U}(f, x) = \mathbb{E}_{y \sim P(\mathcal{Y}|x)} [l(f(x) - y)] \quad (3)$$

This expected loss stems from the random nature of the data  $P(\mathcal{Y}|x)$  (aleatoric uncertainty) as well as prediction errors by the function due to insufficient knowledge (epistemic uncertainty).

**Definition 2** A *Bayes optimal predictor*  $f^*$  is defined as the predictor  $f$  of sufficient capacity that minimizes  $\mathcal{U}$  at every point  $x$ .

$$f^* = \operatorname{argmin}_f \mathcal{U}(f, x) \quad (4)$$

The remaining expected error for a Bayes optimal predictor is defined as the ‘‘aleatoric uncertainty’’.

**Definition 3** The *aleatoric uncertainty*  $\mathcal{A}(\mathcal{Y}|x)$  of some data  $y \sim P(\mathcal{Y}|x)$  is defined as the irreducible uncertainty of a predictor, or the total uncertainty of an *optimal* predictor.

$$\mathcal{A}(\mathcal{Y}|x) = \mathcal{U}(f^*, x) \quad (5)$$

Note that the aleatoric uncertainty is defined over the conditional data distribution, and is not conditioned on the estimator. By definition,  $\mathcal{A}(\mathcal{Y}|x) \leq \mathcal{U}(f, x), \forall f \forall x$ .

**Definition 4** The *variance*  $\sigma^2(\mathcal{Y})$  of some data  $y \sim P(\mathcal{Y})$  is defined as the expected loss of  $y$  against its expected value when  $P(\mathcal{Y})$  is Gaussian.

$$\sigma^2(\mathcal{Y}) = \mathbb{E}_{y_i \sim P(\mathcal{Y})} [l(y_i - \mathbb{E}_{y \sim P(\mathcal{Y})}[y])] \quad (6)$$

For an optimal predictor  $f^*$ , it can be shown that  $\mathcal{U}(f^*, x) = \sigma^2(\mathcal{Y}|x)$  if the loss  $l$  is the squared error loss. Hence, by extension,  $\mathcal{A}(\mathcal{Y}|x) = \sigma^2(\mathcal{Y}|x) = \mathcal{U}(f^*, x)$ .

**Definition 5** The *epistemic uncertainty*  $\mathcal{E}(f, x)$  is defined as the difference between total uncertainty and aleatoric uncertainty. This quantity will asymptotically approach zero as the amount of data goes to infinity for a predictor  $f$  with sufficient capacity.

$$\mathcal{E}(f, x) = \mathcal{U}(f, x) - \mathcal{A}(\mathcal{Y}|x) = \mathcal{U}(f, x) - \mathcal{U}(f^*, x) \quad (7)$$

## 4 Epistemic Uncertainty for Q-value Estimators

Whilst Jain et al. (2021) relate epistemic uncertainty to the one-step Bellman error, we believe it should be related to full trajectories instead due to  $Q$ -values being learned through bootstrapping rather than ground truth targets.

### 4.1 Pathwise Epistemic Uncertainty

In this section, we derive epistemic uncertainty in terms of  $Q$ -value networks for any  $\{\mathbf{s}_t, \mathbf{a}_t\}$  pair. All expectations in this section are taken over  $\mathbf{s}_{t+1}, r_t \sim \rho_{\text{env}}(\cdot|\mathbf{s}_t, \mathbf{a}_t), \mathbf{a}_{t+1} \sim \pi_\theta(\cdot|\mathbf{s}_{t+1})$ .

**Proposition 1** For a  $Q$ -value estimator, the *stepwise total uncertainty* can be defined as the expected total loss for  $Q_\phi^\pi$ :

$$\begin{aligned} \mathcal{U}(Q_\phi^\pi, \{\mathbf{s}_t, \mathbf{a}_t\}) = \\ \mathbb{E}[l(Q_\phi^\pi(\mathbf{s}_t, \mathbf{a}_t) - r_t - \gamma Q_\phi^\pi(\mathbf{s}_{t+1}, \mathbf{a}_{t+1}))] \end{aligned} \quad (8)$$

**Proposition 2** Likewise, we can define *stepwise aleatoric uncertainty* for an estimated  $Q$ -value as the variance in the target  $Q$ -value by extending Eq. (6) for  $Q$ -value predictions:

$$\begin{aligned} \mathcal{A}(Q_\phi^\pi|\{\mathbf{s}_t, \mathbf{a}_t\}) = \\ \mathbb{E}[l(r_t + \gamma Q_\phi^\pi(\mathbf{s}_{t+1}, \mathbf{a}_{t+1}) \\ - \mathbb{E}[r_t + \gamma Q_\phi^\pi(\mathbf{s}_{t+1}, \mathbf{a}_{t+1})])] \end{aligned} \quad (9)$$

**Proposition 3** The *stepwise epistemic uncertainty* for a  $Q$ -value estimator is therefore defined as the difference between the total uncertainty and the aleatoric uncertainty:

$$\begin{aligned} \mathcal{E}_t(Q_\phi^\pi, \{\mathbf{s}_t, \mathbf{a}_t\}) = \\ \mathcal{U}(Q_\phi^\pi, \{\mathbf{s}_t, \mathbf{a}_t\}) - \mathcal{A}(Q_\phi^\pi|\{\mathbf{s}_t, \mathbf{a}_t\}) \end{aligned} \quad (10)$$

**Proposition 4** The stepwise epistemic uncertainty for a  $Q$ -value estimator in a deterministic MDP where  $r_t(\mathbf{s}_t, \mathbf{a}_t) = r_t(\mathbf{s}_t, \mathbf{a}_t, \mathbf{s}_{t+1})$  is equivalent to the Bellman error projected through  $l(\cdot)$ . The proof is given in Appendix A.1.

$$\begin{aligned} \mathcal{E}_t(Q_\phi^\pi, \{\mathbf{s}_t, \mathbf{a}_t\}) \\ = l(Q_\phi^\pi(\mathbf{s}_t, \mathbf{a}_t) - r_t - \gamma \mathbb{E}[Q_\phi^\pi(\mathbf{s}_t, \mathbf{a}_t)]) \\ = l(Q_\phi^\pi(\mathbf{s}_t, \mathbf{a}_t) - r_t - \gamma V_\phi^\pi(\mathbf{s}_t)) \end{aligned} \quad (11)$$

The stepwise epistemic uncertainty merely defines the expected Bellman error for a single  $\{\mathbf{s}_t, \mathbf{a}_t, r_t, \mathbf{s}_{t+1}\}$  transition. In order to obtain a true measure of epistemic uncertainty accounting for the uncertainty in the target measurement, we define a so-called *pathwise epistemic uncertainty*.

**Proposition 5** The *pathwise epistemic uncertainty* for a  $Q$ -value estimator,  $\mathcal{E}_T(Q_\phi^\pi, \{\mathbf{s}_t, \mathbf{a}_t\})$  is the expected cumulative discounted sum of stepwise epistemic uncertainties from the state  $\mathbf{s}_t$  and taking action  $\mathbf{a}_t$ , then performing according to  $\pi$  until the end of the episode.

$$\begin{aligned} \mathcal{E}_T(Q_\phi^\pi, \{\mathbf{s}_t, \mathbf{a}_t\}) = \\ \mathcal{E}_t(Q_\phi^\pi, \{\mathbf{s}_t, \mathbf{a}_t\}) + \gamma \mathbb{E}[\mathcal{E}_T(Q_\phi^\pi, \{\mathbf{s}_{t+1}, \mathbf{a}_{t+1}\})] \end{aligned} \quad (12)$$

In fact, this quantity is a direct estimate of the prediction error of  $Q_\phi^\pi$  at  $\mathbf{s}_t, \mathbf{a}_t$ .

## 4.2 The F-value for Q-value Estimators

In this section, we develop a method for computing an upper bound estimate to the pathwise epistemic uncertainty defined in the previous section for general non-deterministic MDPs, where, in general,  $r_t(\mathbf{s}_t, \mathbf{a}_t, \mathbf{s}_{t+1}) \neq r_t(\mathbf{s}_t, \mathbf{a}_t) \sim P(r_t | \mathbf{s}_t, \mathbf{a}_t)$ . We call this upper bound the  $F$ -value.

**Proposition 6** For a non-deterministic MDP, the upper bound of the stepwise epistemic uncertainty derived in Proposition 4 (which differs from the true value by a constant) can be estimated using Monte Carlo sampling. The corresponding proof is in Appendix A.2, which assumes that the  $Q$ -value is Gaussian. Though restrictive, this is not the first time this assumption has been made (D’Eramo et al. 2021; Chowdhary et al. 2014), and a case in distributional RL has also made this assumption (Clements et al. 2019).

$$\begin{aligned} \mathcal{E}_t(Q_\phi^\pi, \{\mathbf{s}_t, \mathbf{a}_t\}) \\ = \mathbb{E}[l(Q_\phi^\pi(\mathbf{s}_t, \mathbf{a}_t) - r_t - \gamma V_\phi^\pi(\mathbf{s}_{t+1}))] + \sigma^2(r_t) \\ \geq \mathbb{E}[l(Q_\phi^\pi(\mathbf{s}_t, \mathbf{a}_t) - r_t - \gamma V_\phi^\pi(\mathbf{s}_{t+1}))] \end{aligned} \quad (13)$$

**Proposition 7** Following Propositions 5 and 6, the upper bound estimate of the pathwise epistemic uncertainty can be derived as  $F^2(Q_\phi^\pi, \{\mathbf{s}_t, \mathbf{a}_t\})$ , which is semantically equivalent to Eq. (12).

$$\begin{aligned} F^2(Q_\phi^\pi, \{\mathbf{s}_t, \mathbf{a}_t\}) = \\ \mathcal{E}_t(Q_\phi^\pi, \{\mathbf{s}_t, \mathbf{a}_t\}) + \gamma \mathbb{E}[F^2(Q_\phi^\pi, \{\mathbf{s}_{t+1}, \mathbf{a}_{t+1}\})] \end{aligned} \quad (14)$$

**Proposition 8** The  $F$ -value, written as  $F(Q_\phi^\pi, \{\mathbf{s}_t, \mathbf{a}_t\})$ , is simply the standard deviation variant of  $F^2$ .

$$\begin{aligned} F(Q_\phi^\pi, \{\mathbf{s}_t, \mathbf{a}_t\}) = \\ \left( \mathcal{E}_t(Q_\phi^\pi, \{\mathbf{s}_t, \mathbf{a}_t\}) \right. \\ \left. + \gamma \mathbb{E} \left[ \left( F(Q_\phi^\pi, \{\mathbf{s}_{t+1}, \mathbf{a}_{t+1}\}) \right)^2 \right] \right)^{\frac{1}{2}} \end{aligned} \quad (15)$$

To train a model to predict its own  $F$ -value, we propose that the  $Q$ -value network can be trained via bootstrapping to also output an estimate of  $F(Q_\phi^\pi, \{\mathbf{s}_t, \mathbf{a}_t\})$  at the output. Algorithm 1 contains an example implementation of  $F$ -value prediction for DQN.

In summary, we propose that a reasonable measure of epistemic uncertainty for  $Q$ -value networks on  $\{\mathbf{s}_t, \mathbf{a}_t\}$  pairs can be computed by evaluating the quantity in Eq. (15), which is the expected discounted sum of Bellman errors projected through the squared error function in Eq. (13), and that the prediction of this value can be done on a separate output of the  $Q$ -value network itself.

---

### Algorithm 1: Deep Q Network Training with $F$ -value Estimation

---

Select learning rates  $\eta_\phi$  and initialize parameter vector  $\phi$  for learned network  $C_\phi$

**for** number of episodes **do**

Initialize  $\mathbf{s}_t = \mathbf{s}_{t_0} \sim P(\cdot)$

**while** env not done **do**

Get  $Q^\pi$  and  $F$  from learned network  $C_\phi(\mathbf{s}_t)$

Pick  $\mathbf{a}_t$  as  $\operatorname{argmax}_{\mathbf{a}_t} Q^\pi(\mathbf{a}_t)$

Sample  $r_t, \mathbf{s}_{t+1}$  from environment  $\rho_{\text{env}}(\cdot | \mathbf{s}_t, \mathbf{a}_t)$

Store transition tuples  $\{\mathbf{s}_t, \mathbf{a}_t, r_t, \mathbf{s}_{t+1}\}$  in  $\mathcal{D}$

**end while**

**for**  $\{\mathbf{s}_t, \mathbf{a}_t, r_t, \mathbf{s}_{t+1}, \bar{\mathbf{a}}_t\}$  in  $\mathcal{D}$  **do**

Get  $Q^\pi$  and  $F$  from learned network  $C_\phi(\mathbf{s}_t)$

Pick  $\mathbf{a}_t$  as  $\operatorname{argmax}_{\mathbf{a}_t} Q^\pi(\mathbf{a}_t)$

Compute  $Q^{\pi \text{ target}} = (r_t + \gamma Q^\pi(\mathbf{a}_{t+1}))$

Compute  $\mathcal{L}_Q^\pi = l(Q^\pi(\mathbf{a}_t) - Q^{\pi \text{ target}})$

Compute  $F^{\text{target}} = (\mathcal{L}_Q^\pi + \gamma F(\mathbf{a}_{t+1}))^{\frac{1}{2}}$

Compute  $\mathcal{L}_F = l(F(\mathbf{a}_t), F^{\text{target}})$

Update network  $\phi \leftarrow \phi - \eta_\phi \nabla_\phi (\mathcal{L}_Q^\pi + \mathcal{L}_F)$

**end for**

**end for**

---

## 5 Critic Confidence Guided Exploration

In this section, we propose a technique to improve the sample efficiency of RL agents by choosing to mimic an oracle policy when uncertain, and performing self-exploration when the oracle policy’s actions have been explored. In contrast to current techniques where the agent has no control over when to mimic the oracle policy (e.g. annealed weighting in Rosenstein et al. (2004), or random oracle policy walks in Uchendu et al. (2022)), our technique leverages the uncertainty of the agent to control when to follow the oracle policy. This method circumvents the issue where the learning policy is unlikely to see the oracle’s actions in regions of the environment that are unreachable by the oracle policy.

### 5.1 A New Approach to Improving Sample Efficiency

Our method of improving sample efficiency with an oracle policy is loosely inspired by UCB (Auer 2002). Assume that we have a critic  $Q_\phi^\pi$  and means of computing a measure of its likely prediction error  $e_\phi$ . When presented with a state and action  $\{\mathbf{s}_t, \mathbf{a}_t\}$ , we can assign an upperbound to the true  $Q^\pi$  value as in Eq. (16).

$$\Lambda(Q^\pi, \{\mathbf{s}_t, \mathbf{a}_t\}) = Q_\phi^\pi(\mathbf{s}_t, \mathbf{a}_t) + e_\phi(\mathbf{s}_t, \mathbf{a}_t) \quad (16)$$

Thus, when we also have the action of the oracle policy  $\bar{\mathbf{a}}_t$ , it is now possible to evaluate the potential improvement in the  $Q$ -value by following the action of the oracle versus that of the learning policy.

$$\begin{aligned} \Delta(Q^\pi, \{\mathbf{s}_t, \mathbf{a}_t, \bar{\mathbf{a}}_t\}) = \\ \Lambda(Q^\pi, \{\mathbf{s}_t, \bar{\mathbf{a}}_t\}) - \Lambda(Q^\pi, \{\mathbf{s}_t, \mathbf{a}_t\}) \end{aligned} \quad (17)$$

To utilize this measure to guide supervision, we first define the supervision loss for continuous action spaces as

$$\mathcal{L}_{\text{sup}}(\pi_\theta) = \mathbb{E}_{\substack{\mathbf{a}_t \sim \pi_\theta(\cdot | \mathbf{s}_t) \\ \bar{\mathbf{a}}_t \sim \bar{\pi}(\cdot | \mathbf{s}_t)}} [ \|\mathbf{a}_t - \bar{\mathbf{a}}_t\|_2^2 ] \quad (18)$$

which is simply the expected squared error loss between the actor-sampled action and the oracle-provided action. That said, any other loss function used in supervised learning in similar contexts can be used, such as minimizing the negative log likelihood  $-\log \pi_\theta(\bar{\mathbf{a}}_t)$ , L1 loss function  $|\mathbf{a}_t - \bar{\mathbf{a}}_t|$ , or similar. Discrete action space models can instead utilize the cross entropy loss  $-\bar{\mathbf{a}}_t \log(\pi(\mathbf{a}_t))$ .

The loss function of the actor for observation  $\mathbf{s}_t$  is then formulated as a convex combination of a supervisory signal from Eq. (18) and a reinforcement signal from Eq. (2):

$$\begin{aligned} \mathcal{L}_{\text{CCGE}} = & \\ & \mathbb{E}_{\substack{\mathbf{a}_t \sim \pi_\theta(\cdot | \mathbf{s}_t) \\ \bar{\mathbf{a}}_t \sim \bar{\pi}(\cdot | \mathbf{s}_t)}} [ k([\lambda_{\text{sup}} \|\mathbf{a}_t - \bar{\mathbf{a}}_t\|_2^2]) \\ & + (1 - k)(-[Q_\phi^\pi(\mathbf{s}_t, \mathbf{a}_t)]) ] \end{aligned} \quad (19)$$

where  $\lambda_{\text{sup}}$  is a scaling constant whilst  $k$  is computed with:

$$k = \text{clamp} \left( \frac{\Delta(Q^\pi, \{\mathbf{s}_t, \mathbf{a}_t, \bar{\mathbf{a}}_t\})}{Q_\phi^\pi(\mathbf{s}_t, \mathbf{a}_t)} \cdot \lambda_{\text{conf}} \right) \in (0, 1) \quad (20)$$

where  $\lambda_{\text{conf}}$  is a scaling constant which we term *confidence scale* and clamp simply limits the output to  $[0, 1]$ . To put simply, the tradeoff between the learning policy imitating the oracle policy versus performing reinforcement learning is scaled according to the normalized potential gain of following the former versus the latter.

## 5.2 Utilizing F-values

We build off SAC and the core idea of critic uncertainty estimation to realize the idea presented in the previous section. We propose using the  $F$ -value as a proxy for computing  $e_\phi$ . Therefore,

$$\Lambda(Q^\pi, \{\mathbf{s}_t, \mathbf{a}_t\}) = Q_\phi^\pi(\mathbf{s}_t, \mathbf{a}_t) + F(Q_\phi^\pi, \{\mathbf{s}_t, \mathbf{a}_t\}) \quad (21)$$

Unfortunately, we may not have good estimates for  $\Lambda(Q_\phi^\pi, \{\mathbf{s}_t, \bar{\mathbf{a}}_t\})$  in out-of-distribution data. One workaround that introduces additional machinery is to utilize Normalizing Flows (Rezende and Mohamed 2015) and force high  $F$ -values for out-of-distribution data and regress to known values for in-distribution data. Instead, we propose a benefit-of-doubt approach to measuring  $\Delta(Q^\pi, \{\mathbf{s}_t, \mathbf{a}_t, \bar{\mathbf{a}}_t\})$ .

In SAC, an ensemble of  $n(=2)$   $Q$ -value networks are used to tame overestimation bias (Van Hasselt, Guez, and Silver 2016; Haarnoja et al. 2018b). If each  $Q$ -value network also performed  $F$ -value prediction, we conveniently have an ensemble of  $F$ -value predictors. We thus have  $\Lambda_i(Q^\pi, \{\mathbf{s}_t, \mathbf{a}_t\})$  for  $i \in \{0, 1, \dots, n-1\}$  per  $\{\mathbf{s}_t, \mathbf{a}_t\}$  pair. We then propose intentionally overestimating  $\Delta(Q^\pi, \{\mathbf{s}_t, \mathbf{a}_t, \bar{\mathbf{a}}_t\})$  by taking the maximal difference according to the ensemble:

$$\begin{aligned} \Delta(Q^\pi, \{\mathbf{s}_t, \mathbf{a}_t, \bar{\mathbf{a}}_t\}) = & \\ & \max_i [\Lambda_i(Q^\pi, \{\mathbf{s}_t, \bar{\mathbf{a}}_t\})] - \min_i [\Lambda_i(Q^\pi, \{\mathbf{s}_t, \mathbf{a}_t\})] \end{aligned} \quad (22)$$

Eq. (22) is then used in Eq. (20) to close Eq. (19), which concludes our Critic Confidence Guided Exploration (CCGE) algorithm. In our experiments, we find it beneficial to artificially bias the  $F$ -value branches with a random weight between 1-100. This has the effect of exaggerating the supervision scale in the beginning of training, improving model performance in some cases. The complete algorithm for CCGE is shown in Algorithm 2.

---

Algorithm 2: Critic Confidence Guided Exploration (CCGE) using  $F$ -values

---

Select discount factor  $\gamma$ , learning rates  $\eta_\phi, \eta_\pi$   
 Select size of  $Q$ -value network ensemble  $n$   
 Select CCGE hyperparameters  $\lambda_{\text{conf}}$  and  $\lambda_{\text{sup}}$

Initialize parameter vectors  $\theta, \phi_i$  for  $i \in \{0, \dots, n-1\}$   
 Initialize actor and critic networks  $\pi_\theta, C_{\phi_i}$  for  $i \in \{0, \dots, n-1\}$   
 Initialize or hardcode oracle  $\bar{\pi}$

**for** number of episodes **do**

Initialize  $\mathbf{s}_t = \mathbf{s}_{t=0} \sim P(\cdot)$

**while** env not done **do**

Sample  $\mathbf{a}_t$  from  $\pi(\cdot | \mathbf{s}_t)$

Sample  $\bar{\mathbf{a}}_t$  from  $\bar{\pi}(\cdot | \mathbf{s}_t)$

Sample  $r_t, \mathbf{s}_{t+1}$  from  $\rho_{\text{env}}(\cdot | \mathbf{s}_t, \mathbf{a}_t)$

Store transition tuples  $\{\mathbf{s}_t, \mathbf{a}_t, r_t, \mathbf{s}_{t+1}, \bar{\mathbf{a}}_t\}$  in  $\mathcal{D}$

**end while**

**for**  $\{\mathbf{s}_t, \mathbf{a}_t, r_t, \mathbf{s}_{t+1}, \bar{\mathbf{a}}_t\}$  in  $\mathcal{D}$  **do**

Get  $Q_{\phi_i}^\pi, F_{\phi_i}$  from each critic  $C_{\phi_i}(\mathbf{s}_t, \mathbf{a}_t)$

Compute  $Q^{\pi^{\text{target}}} = r_t + \gamma \min_i Q_{\phi_i}^\pi$

Compute  $\mathcal{L}_{Q_i^\pi} = l(Q_{\phi_i}^\pi - Q^{\pi^{\text{target}}}) \quad \forall i$

Compute  $F^{\text{target}} = (\min_i \mathcal{L}_{Q_i^\pi} + \gamma(\min_i F_{\phi_i}))^{\frac{1}{2}}$

Compute  $\mathcal{L}_{F_i} = l(F_{\phi_i} - F^{\text{target}}) \quad \forall i$

Update critics  $\phi_i \leftarrow \phi_i - \eta_\phi \nabla_{\phi_i} (\mathcal{L}_{Q_i^\pi} + \mathcal{L}_{F_i})$

Update actor  $\theta \leftarrow \theta - \eta_\theta \nabla_\theta \mathcal{L}_{\text{CCGE}}$

**end for**

**end for**

---

## 6 Experimental Work

We implement the  $F$ -value estimation as in Eq. (15) on two off-policy algorithms, namely SAC and DQN. We then evaluate their behavior and performance in a variety of environments, from continuous control tasks to domain-randomized image-based observation environments available from Gym (Brockman et al. 2016) and PyBullet Gym (Ellenberger 2018–2019) libraries. Following guidelines from RLiable (Agarwal et al. 2021), we report 50% interquartile means (IQM) with bootstrapped confidence intervals. Our experiments aim to answer the following questions:

1. How does the  $F$ -value behave during learning?
2. What does the  $F$ -value tell us about the learning process?

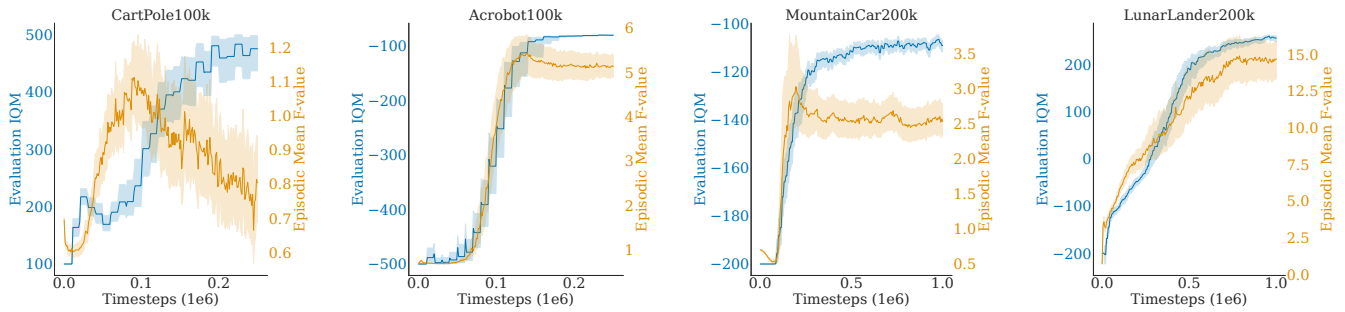


Figure 1: Aggregate  $F$ -value and evaluation scores across four environments using DQN with  $F$ -value prediction.

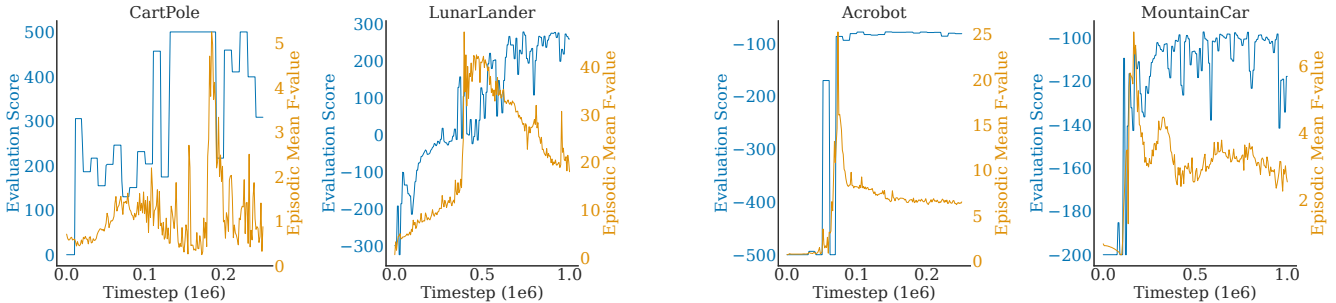


Figure 2:  $F$ -value example on non-sparse reward environments using DQN with  $F$ -value prediction.

Figure 3:  $F$ -value example on sparse reward environments using DQN with  $F$ -value prediction.

3. How does the  $F$ -value react to out of distribution data?
4. How does CCGE perform on continuous control robotics tasks?
5. How does CCGE affect learning in hyperparameter sensitive settings?

All relevant source code is available online<sup>1</sup>, and all relevant hyperparameters are listed in Appendix E.

## 6.1 Analysis of $F$ -value

**How does the  $F$ -value behave during learning?** We implement DQN with  $F$ -value estimation on four environments from Gym with increasing difficulty and complexity (Brockman et al. 2016): CartPole, Acrobot, MountainCar, and LunarLander. We aggregate results over 150 runs using varying hyperparameters (see Appendix E).

On CartPole in Fig. 1, the  $F$ -value indicates that model uncertainty starts small, increases and then decreases, while evaluation performance exhibits a mostly upward trend. This is perhaps expected, since state diversity –and therefore reward diversity– start small and increase during training, model uncertainty follows the same initial trend. Eventually, model uncertainty falls as  $Q$ -value predictions get more accurate through sufficient exploration and  $Q$ -value network updates, leading to better performance and lower model uncertainties. This trend is similarly observed in Acrobot and MountainCar, albeit to a lesser extent. Conversely, it is not observed for the more challenging LunarLander, where the

trend of the  $F$ -value increases monotonically and plateaus out in aggregate. More results using different replay buffer sizes are shown in Appendix C.

**What does the  $F$ -value tell us about the learning process?** In environments with rewards that vary fairly smoothly such as CartPole and LunarLander (Figure 2(a)), the  $F$ -value can show either performance collapse as in the example shown in CartPole, or indicate state exploration activity as in LunarLander. In environments with sparse rewards such as Acrobot and MountainCar (Figure 2(b)), the  $F$ -value is indicative of agent learning progress: we observe spikes in uncertainty when the model discovers crucial checkpoints in the environment. For Acrobot, this occurs when the upright position is reached and the reward penalty is stopped. In MountainCar, this occurs when the agent first reaches the top of the mountain, which completes the environment. More examples of similar plots are shown in Appendix D.

## 6.2 Critic Confidence Guided Supervision Performance Analysis

**How does the  $F$ -value react to out of distribution data?** Our implementations of  $F$ -value estimation make no consideration for estimation on out-of-distribution data. Nevertheless, we aim to study how DQN predicts  $F$ -values for observations it has not seen before. We implement DQN with  $F$ -value prediction in the discrete version of CarRacing from Gym, and train for  $10^5$  timesteps before performing a domain change by changing the colors of the environment.

<sup>1</sup>link available soon

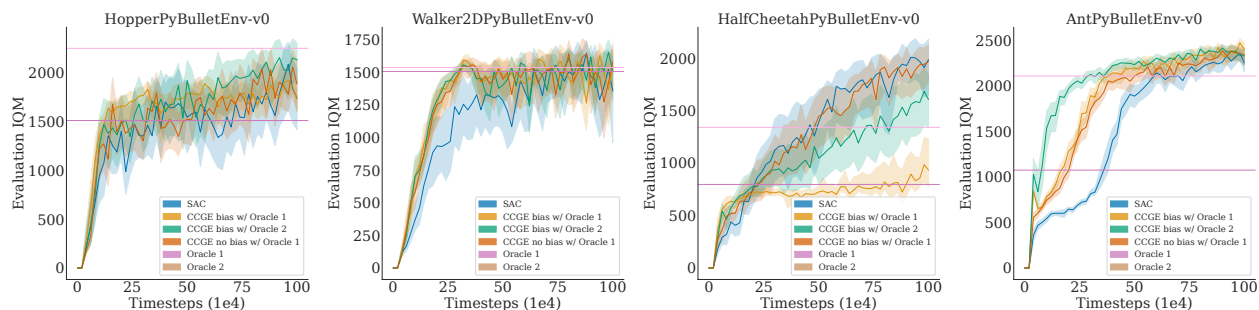


Figure 4: Learning curves of CCGE and SAC on PyBullet tasks. The line denotes the mean over 35 runs and evaluation performance is the total episodic reward over 20 episodes.

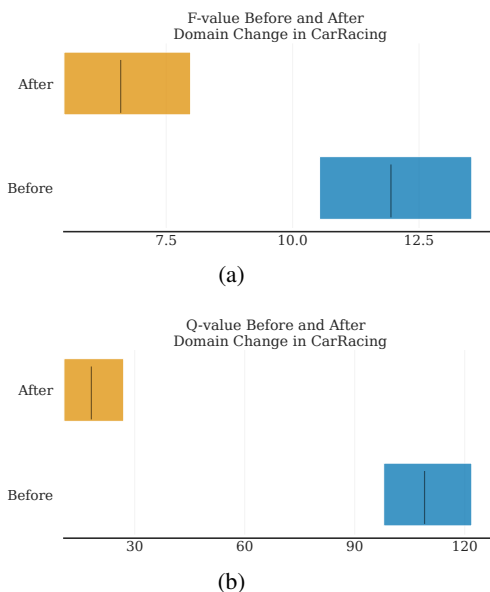


Figure 5: Model predicted (a)  $F$ -value and (b)  $Q$ -value before and after domain change on CarRacing.

This domain change generates unseen observations, resulting in the model making predictions on out-of-distribution data. We record the mean episodic  $F$ - and  $Q$ -values across 50 runs before and after the domain change and plot 50% interquartile means of all recorded values in Fig. 5.

We see that the predicted  $F$ -values actually fall after the domain change. This may seem counter-intuitive, but observing the corresponding distribution of  $Q$ -values before and after the change shows that the predicted  $Q$ -values also fall correspondingly. This suggests that, while uncertainty may have fallen, it could be due to the model correctly assessing that its performance is likely bad. Furthermore, while both values fall, the ratio between  $F$ - and  $Q$ -values actually increases, possibly hinting that there is merit in studying the value of  $F/Q$  instead.

**How does CCGE perform on continuous control robotics tasks?** We implement CCGE on four standard continuous control robotics RL benchmarks: Hopper, Walker,

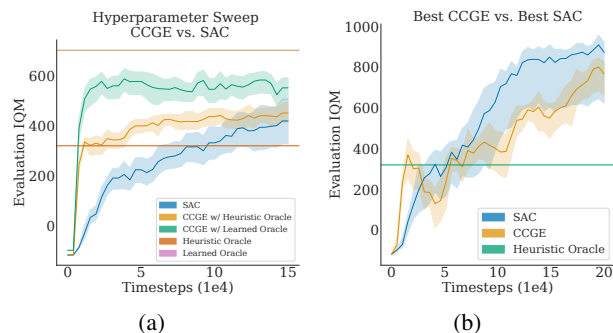


Figure 6: Learning curves of CCGE and SAC on domain-randomized CarRacing. a) Each line denotes 50 runs over a set of hyperparameters. b) Each line denotes 10 runs using the best performing hyperparameters taken from the sweep done in a).

HalfCheetah, and Ant from PyBullet-Gym (Ellenberger 2018–2019) using optimized hyperparameters taken from Raffin, Kober, and Stulp (2022). We compare the performance of CCGE using two different oracles (which we call Oracle 1 and Oracle 2) of differing performance against SAC. Both oracle policies have 100 neurons per layer as opposed to  $\geq 300$  of the learning policy and are trained using SAC. Oracle 1 is trained with 10% of the total timesteps of the learning policy, while Oracle 2 uses 50% of the total timesteps of the learning policy. With Oracle 2, we perform separate runs with and without the artificial bias described in Section 5.2. The learning curves for the four environments and two algorithms are shown in Fig. 4.

With the exception of HalfCheetah, CCGE performs similarly or better than SAC in both sample efficiency and final performance. This is especially evident in the Ant environment. Curiously, in HalfCheetah, the presence of the oracle policy frequently locks the learning policy into the local optimum of favouring standing still. Considering that CCGE reduces the amount of exploration done in the environment, this can be an expected behaviour and hints towards the need for careful selection of an oracle policy.

**How does CCGE affect learning in hyperparameter sensitive settings?** Our aim is to study how CCGE influences agent learning in environments where only a small subset of hyperparameters allow effective learning through SAC. To this end, we apply SAC and CCGE with artificial bias to the continuous action space CarRacing environment from Gym with the domain randomization flag enabled. The evaluation metric we use is the mean episodic total reward over 50 episodes. Again, we utilize two different oracle policies. The first oracle policy uses a hardcoded heuristic policy which adjusts the steering angle according to the track angle relative to the car. The second oracle policy uses the best-performing policy obtained from CCGE using the first oracle policy. We run 50 experiments each using SAC and CCGE with hyperparameters randomly sampled from a set of reasonable defaults.

In this context, CCGE demonstrates a reduction in overall learning variance and better average performance when compared to SAC (shown in Fig. 6(a)). More crucially, all instances of CCGE using the first oracle policy learn some meaningful behavior of moving forward, achieving a score of at least 300. In contrast, seven out of 50 runs in SAC achieve scores lower than 300, with three of those favouring staying still with an evaluation score of lower than -50.0. In the case of CCGE using the second oracle policy, the minimum score achieved was 517.

When using the best hyperparameters as shown in Fig. 6(b), SAC still outperforms CCGE. We believe that CCGE’s policy reverts to the oracle policy whenever it encounters uncertain observations, which happens often in the domain-randomized variant of CarRacing. This is especially evident in the occasional dip in performance for CCGE.

## 7 Conclusion

In this paper, we proposed and developed a theoretical quantity to evaluate epistemic uncertainty in value-based RL, which we termed *pathwise epistemic uncertainty*:  $\mathcal{E}_T(Q_\phi^\pi, \{\mathbf{s}_t, \mathbf{a}_t\})$ . We drew a connection between this quantity and the conventional Bellman error, and presented a theoretical formulation of its upper bound, which we called the  $F$ -value. In some contexts, the  $F$ -value of a model is observed to provide an interesting insight towards an agent’s learning progress in the environment. We then proposed a new algorithm called *Critic Confidence Guided Exploration* (CCGE) to improve the sample efficiency of actor critic RL algorithms by choosing to learn from an oracle policy depending on the uncertainty of the critic. We further show that it is possible to use the  $F$ -value in CCGE, and that doing so may result in superior sample efficiency, final performance, and learning variance for a set of RL benchmark tasks. Such a form of guided exploration also allows bootstrapped learning, where trained agents can be used as oracles for training newer, more performant agents. In the future, we believe it would be interesting to explore  $F$ -value estimation models that also work for out-of-distribution data, as well as the possibilities of guided exploration in the multi-agent RL setting, which is specifically motivated by humans’ profound ability to leverage other humans as oracles.

## A Stepwise Epistemic Uncertainty in Deterministic and Non-deterministic MDPs

### A.1 Deterministic MDP

In the deterministic MDP case, we assume that  $r_t = r_t(\mathbf{s}_t, \mathbf{a}_t) = r_t(\mathbf{s}_t, \mathbf{a}_t, \mathbf{s}_{t+1})$ , hence  $\mathbb{E}[r_t] = r_t$  and  $\sigma^2(r_t) = 0$  for a given  $(\mathbf{s}_t, \mathbf{a}_t)$  pair.

$$\begin{aligned} \mathcal{E}_t(Q_\phi^\pi, \{\mathbf{s}_t, \mathbf{a}_t\}) &= \mathcal{U}(Q_\phi^\pi, \{\mathbf{s}_t, \mathbf{a}_t\}) - \mathcal{A}(Q_\phi^\pi | \{\mathbf{s}_t, \mathbf{a}_t\}) \\ &= \mathcal{U}(Q_\phi^\pi, \{\mathbf{s}_t, \mathbf{a}_t\}) - \sigma^2(Q_\phi^\pi(\mathbf{s}_t, \mathbf{a}_t)) \\ &= \mathbb{E}[l(Q_\phi^\pi(\mathbf{s}_t, \mathbf{a}_t) - Q^{\pi^{\text{target}}}(\mathbf{s}_t, \mathbf{a}_t))] - \sigma^2(Q_\phi^\pi(\mathbf{s}_t, \mathbf{a}_t)) \\ &= \mathbb{E}[l(Q_\phi^\pi(\mathbf{s}_t, \mathbf{a}_t) - \mathbb{E}[r_t + \gamma Q_\phi^\pi(\mathbf{s}_{t+1}, \mathbf{a}_{t+1})])] \\ &\quad - \sigma^2(Q_\phi^\pi(\mathbf{s}_t, \mathbf{a}_t)) \end{aligned} \quad (23)$$

Using the standard definition of variance of  $\sigma^2(x) = \mathbb{E}[l(x)] - l(\mathbb{E}(x))$ , we can break down the first term into:

$$\begin{aligned} \mathbb{E}[l(Q_\phi^\pi(\mathbf{s}_t, \mathbf{a}_t) - \mathbb{E}[r_t + \gamma Q_\phi^\pi(\mathbf{s}_{t+1}, \mathbf{a}_{t+1})])] &= \sigma^2(Q_\phi^\pi(\mathbf{s}_t, \mathbf{a}_t) - \mathbb{E}[r_t + \gamma Q_\phi^\pi(\mathbf{s}_{t+1}, \mathbf{a}_{t+1})]) \\ &\quad + l(\mathbb{E}[Q_\phi^\pi(\mathbf{s}_t, \mathbf{a}_t) - \mathbb{E}[r_t + \gamma Q_\phi^\pi(\mathbf{s}_{t+1}, \mathbf{a}_{t+1})]]) \\ &= \sigma^2(Q_\phi^\pi(\mathbf{s}_t, \mathbf{a}_t) - \mathbb{E}[r_t + \gamma Q_\phi^\pi(\mathbf{s}_{t+1}, \mathbf{a}_{t+1})]) \\ &\quad + l(Q_\phi^\pi(\mathbf{s}_t, \mathbf{a}_t) - \mathbb{E}[r_t + \gamma Q_\phi^\pi(\mathbf{s}_{t+1}, \mathbf{a}_{t+1})]) \\ &= \sigma^2(Q_\phi^\pi(\mathbf{s}_t, \mathbf{a}_t)) \\ &\quad + l(Q_\phi^\pi(\mathbf{s}_t, \mathbf{a}_t) - \mathbb{E}[r_t + \gamma Q_\phi^\pi(\mathbf{s}_{t+1}, \mathbf{a}_{t+1})]) \end{aligned} \quad (24)$$

The final term arises because  $\sigma^2(x + C) = \sigma^2(x)$  where  $C$  is a constant. Finally, substituting Eq. 24 into Eq. 23, we obtain:

$$\begin{aligned} \mathcal{E}_t(Q_\phi^\pi, (\mathbf{s}_t, \mathbf{a}_t)) &= \sigma^2(Q_\phi^\pi(\mathbf{s}_t, \mathbf{a}_t)) + l(Q_\phi^\pi(\mathbf{s}_t, \mathbf{a}_t) \\ &\quad - \mathbb{E}[r_t + \gamma Q_\phi^\pi(\mathbf{s}_{t+1}, \mathbf{a}_{t+1})]) - \sigma^2(Q_\phi^\pi(\mathbf{s}_t, \mathbf{a}_t)) \\ &= l(Q_\phi^\pi(\mathbf{s}_t, \mathbf{a}_t) - \mathbb{E}[r_t + \gamma Q_\phi^\pi(\mathbf{s}_{t+1}, \mathbf{a}_{t+1})]) \\ &= l(Q_\phi^\pi(\mathbf{s}_t, \mathbf{a}_t) - \mathbb{E}[r_t + \gamma Q_\phi^\pi(\mathbf{s}_{t+1}, \mathbf{a}_{t+1})]) \\ &= l(Q_\phi^\pi(\mathbf{s}_t, \mathbf{a}_t) - r_t - \gamma \mathbb{E}[Q_\phi^\pi(\mathbf{s}_{t+1}, \mathbf{a}_{t+1})]) \\ &= l(Q_\phi^\pi(\mathbf{s}_t, \mathbf{a}_t) - r_t - \gamma V_\phi^\pi(\mathbf{s}_{t+1})) \end{aligned} \quad (25)$$

### A.2 Non-Deterministic MDP

For non-deterministic MDPs, we can show that:

$$\begin{aligned} \mathcal{E}_t(Q_\phi^\pi, (\mathbf{s}_t, \mathbf{a}_t)) &= l(Q_\phi^\pi(\mathbf{s}_t, \mathbf{a}_t), \mathbb{E}[r_t + \gamma Q_\phi^\pi(\mathbf{s}_{t+1}, \mathbf{a}_{t+1})]) \\ &= l(Q_\phi^\pi(\mathbf{s}_t, \mathbf{a}_t), \mathbb{E}[r_t] + \gamma V_\phi^\pi(\mathbf{s}_{t+1})) \\ &= l(Q_\phi^\pi(\mathbf{s}_t, \mathbf{a}_t) - \mathbb{E}[r_t] - \gamma V_\phi^\pi(\mathbf{s}_{t+1})) \\ &= l(\mathbb{E}[Q_\phi^\pi(\mathbf{s}_t, \mathbf{a}_t) - r_t - \gamma V_\phi^\pi(\mathbf{s}_{t+1})]) \\ &\leq \mathbb{E}[l(Q_\phi^\pi(\mathbf{s}_t, \mathbf{a}_t) - r_t - \gamma V_\phi^\pi(\mathbf{s}_{t+1}))] \end{aligned} \quad (26)$$

The last line in the above equation is a measure of epistemic uncertainty for  $Q$ -value estimators in non-deterministic MDP that can be approximated using Monte



Carlo sampling as is normal for deep RL methods. We can further show that this value differs from the MDP case by up to a constant  $\sigma^2(r_t)$  through:

$$\begin{aligned}
 & \mathbb{E}[l(Q_\phi^\pi(\mathbf{s}_t, \mathbf{a}_t) - r_t - \gamma V_\phi^\pi(\mathbf{s}_{t+1}))] \\
 &= l(\mathbb{E}[Q_\phi^\pi(\mathbf{s}_t, \mathbf{a}_t) - r_t - \gamma V_\phi^\pi(\mathbf{s}_{t+1})]) \\
 & \quad + \sigma^2[l(Q_\phi^\pi(\mathbf{s}_t, \mathbf{a}_t) - r_t - \gamma V_\phi^\pi(\mathbf{s}_{t+1}))] \\
 &= l(\mathbb{E}[Q_\phi^\pi(\mathbf{s}_t, \mathbf{a}_t) - r_t - \gamma V_\phi^\pi(\mathbf{s}_{t+1})]) + \sigma^2(r_t)
 \end{aligned} \tag{27}$$

Therefore, in the general case of non-deterministic MDPs, for a Bayes optimal  $Q$ -value estimator, the epistemic uncertainty of the  $Q$ -value estimator can only be measured down to a constant  $\sigma^2(r_t)$ . It is possible to learn a model over  $r_t \sim P(\cdot | \mathbf{s}_t, \mathbf{a}_t)$  that can learn this variance, although this is not done in the present work.

## B Compute

All our experiments run comfortably on a single GPU, and for most cases, we run multiple experiments concurrently in parallel processes on the same GPU. For CarRacing experiments, we utilize Nvidia A100 GPUs. For all other experiments, we use Nvidia GPUs of the following types: GTX 1080Ti, GTX 1060 6G, RTX 3080. All the machines used have a minimum of 16 GB of RAM and 8 CPU threads. Training time heavily depends on the CPU specification and type of GPU used, but all experiments complete in under 24 hours, and in most instances they complete under 12 hours.

## C $F$ -value against Evaluation Performance Aggregate Runs

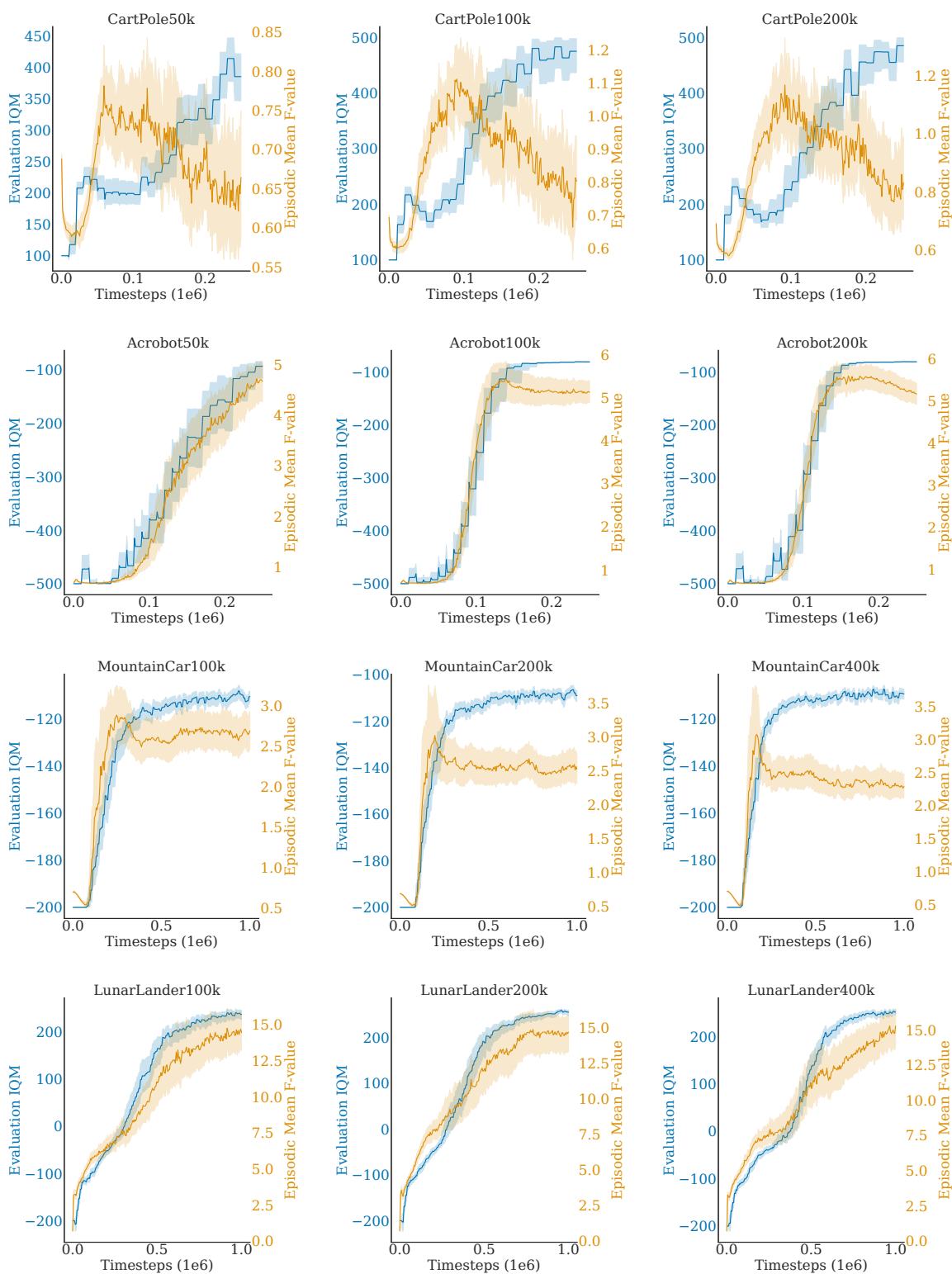


Figure 7: Mean Episodic  $F$ -value and evaluation performance curves for CartPole, Acrobot, MountainCar and LunarLander environments. The number at the end of the environment name in each sub-figure title indicates the size of the replay buffer.

## D Example Individual $F$ -value Curves on Various Runs

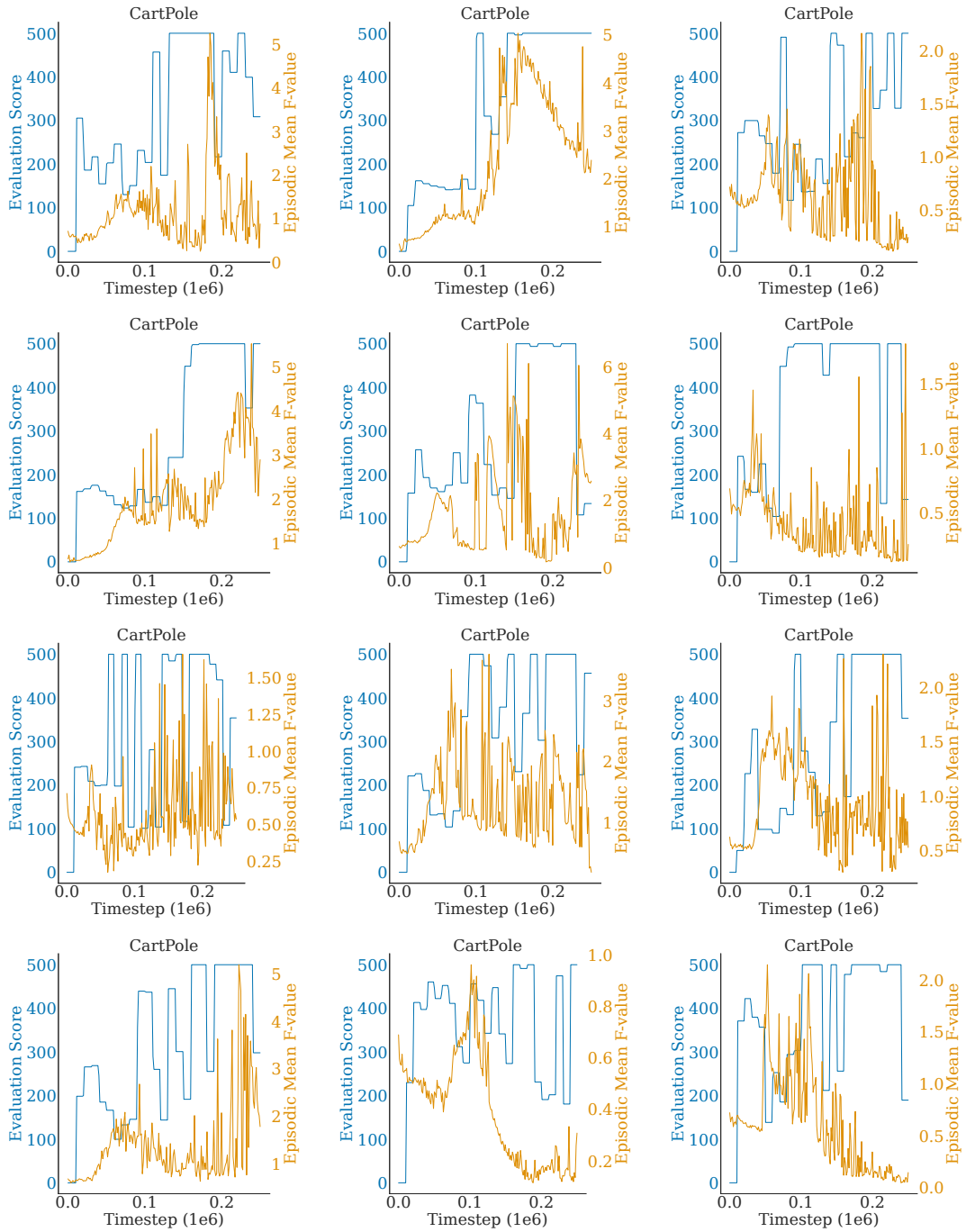


Figure 8: Mean Episodic  $F$ -value and evaluation performance curves on various runs of CartPole.

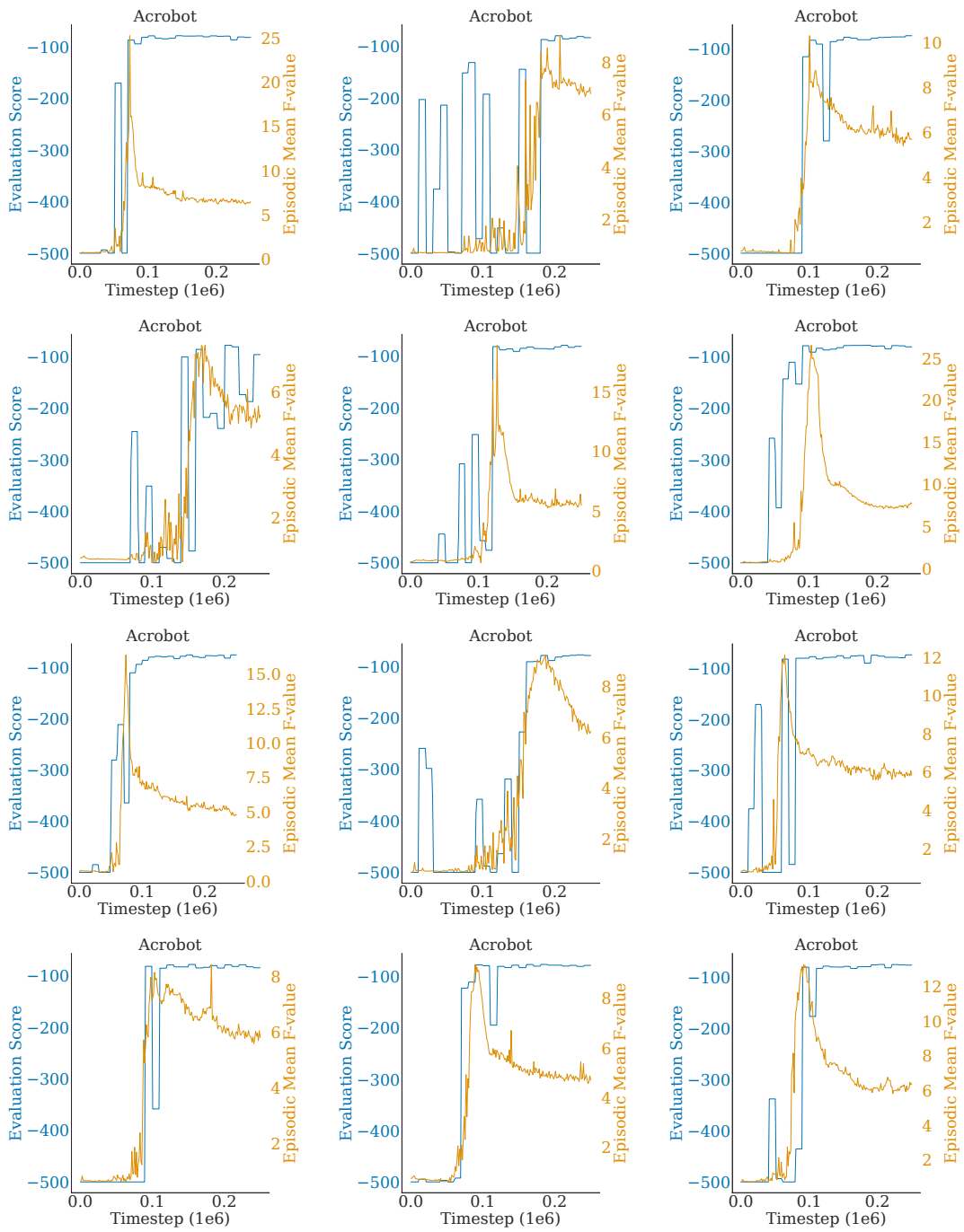


Figure 9: Mean Episodic  $F$ -value and evaluation performance curves on various runs of Acrobot.

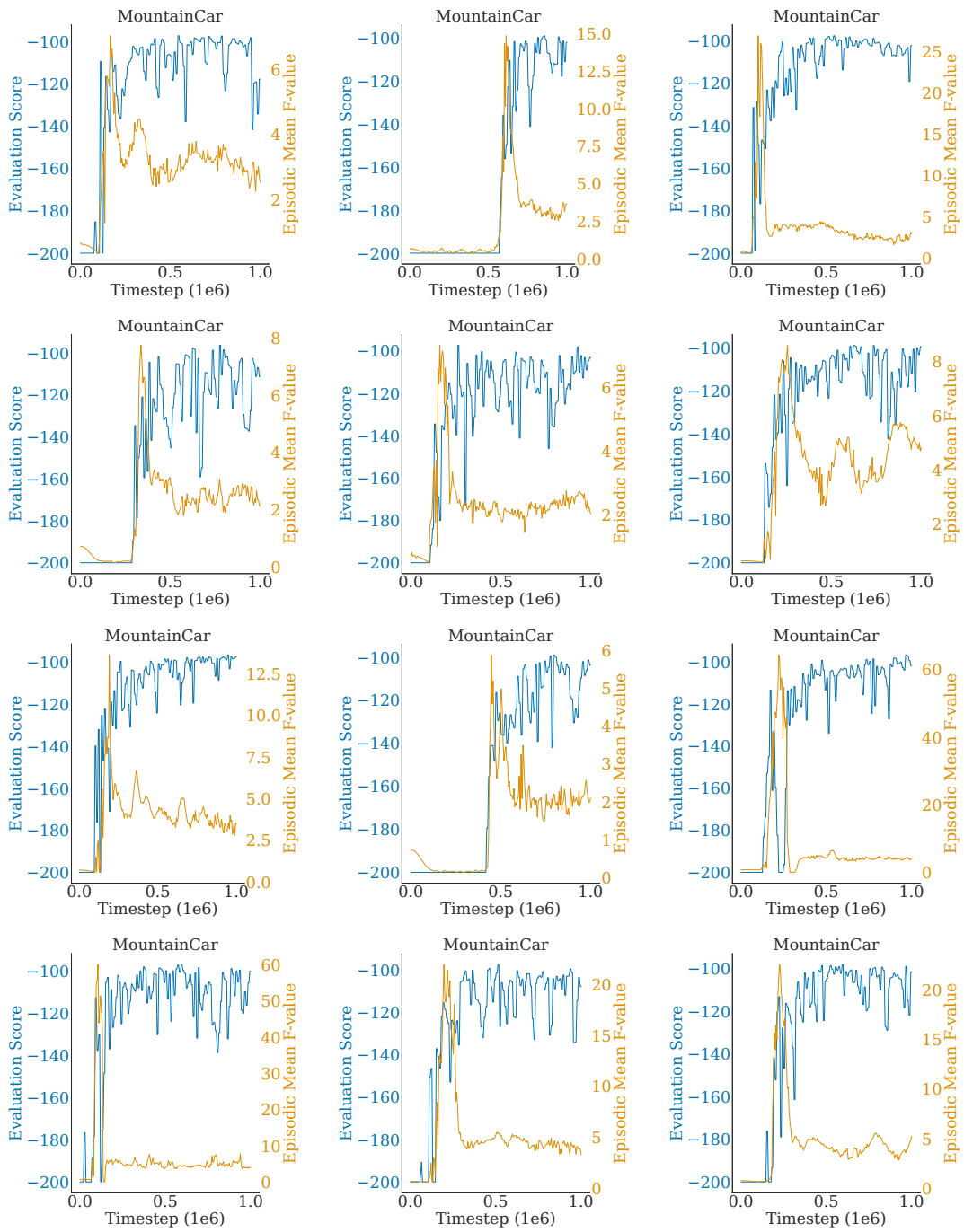


Figure 10: Mean Episodic  $F$ -value and evaluation performance curves on various runs of MountainCar.

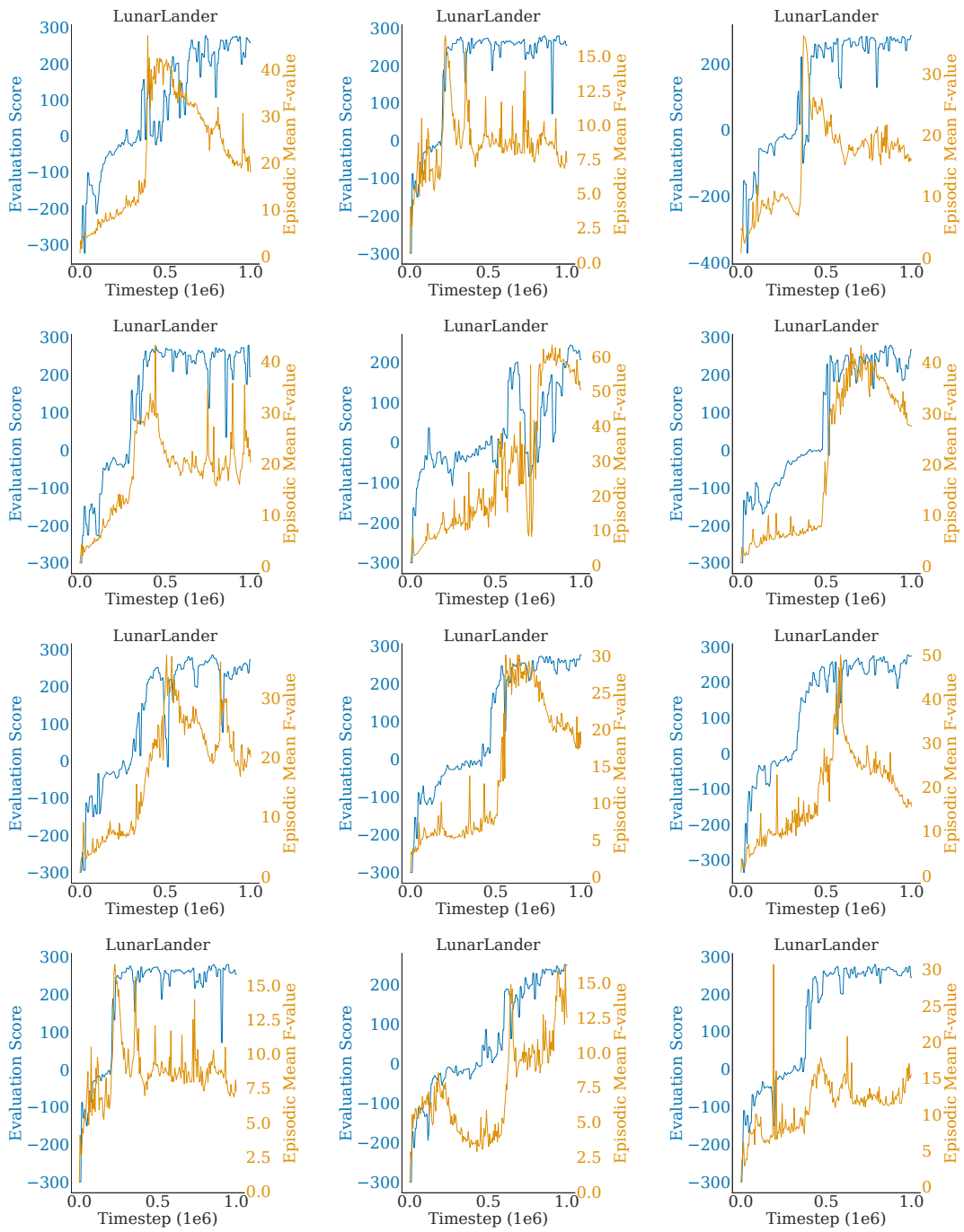


Figure 11: Mean Episodic  $F$ -value and evaluation performance curves on various runs of LunarLander.

## E Hyperparameters

### E.1 DQN Hyperparameters for CartPole, Acrobot, MountainCar and Lunarlander

Table 1: DQN Hyperparameters for CartPole, Acrobot, MountainCar and Lunarlander

Parameter	Value
<i>Constants</i>	
optimizer	AdamW (Loshchilov and Hutter 2018; Kingma and Ba 2015)
number of hidden layers (all networks)	2
number of neurons per layer (all networks)	64
non-linearity	<i>ReLU</i>
number of evaluation episodes	50
evaluation frequency	every $10 \times 10^3$ steps
<i>replay buffer size</i>	
CartPole	$250 \times 10^3$
Acrobot	$250 \times 10^3$
MountainCar	$1 \times 10^6$
LunarLander	$1 \times 10^6$
<i>Ranges</i>	
minibatch size	{128, 256, 512}
max gradient norm	[0.25, 1.00]
learning rate	[0.0001, 0.001]
exploration ratio	[0.05, 0.15]
discount factor	[0.980, 0.999]
gradient steps before target network update	[500, 2000]

### E.2 DQN Hyperparameters for CarRacing

Table 2: DQN Hyperparameters for CarRacing

Parameter	Value
<i>Constants</i>	
<i>DQN Architecture</i>	
Convnet backbone	$[3 \times 3 \text{ conv}, 2 \times 2 \text{ maxpool, non-linearity}] \times 4 + [\text{flatten}]$
Convnet number of kernels	[32, 64, 128, 8]
<i>MLP head</i>	
number of hidden layers	1
number of neurons per layer	128
non-linearity	Leaky <i>ReLU</i>
optimizer	AdamW (Loshchilov and Hutter 2018; Kingma and Ba 2015)
minibatch size	300
number of evaluation episodes	20
evaluation frequency	every $5 \times 10^3$ steps
total steps	$100 \times 10^3$
replay buffer size	$30 \times 10^3$
environment colour change	after $50 \times 10^3$ steps
image size	$3 \times 64 \times 64$
starting frame skips	50
framestack	4
<i>Ranges</i>	
max gradient norm	[0.25, 1.00]
learning rate	[0.0001, 0.001]
exploration ratio	[0.05, 0.15]
discount factor	[0.980, 0.999]
gradient steps before target network update	[500, 2000]

### E.3 CCGE and SAC Hyperparameters for PyBulletEnv

Table 3: CCGE and SAC hyperparameters for PyBulletEnv experiments.

Parameter	Value
<i>Constants</i>	
optimizer	AdamW (Loshchilov and Hutter 2018; Kingma and Ba 2015)
discount( $\gamma$ )	0.98
size of Q ensemble	2
non-linearity	<i>ReLU</i>
target smoothing coefficient ( $\tau$ )	0.005
minibatch size	256
entropy coefficient ( $\alpha$ )	auto
target entropy	$-\dim(\mathbf{A})$
train frequency	episodic
number of evaluation episodes	20
evaluation frequency	every $50 \times 10^3$ steps
<i>CCGE and SAC</i>	
number of hidden layers (all networks)	2
number of neurons per layer	[400, 300]
replay buffer size	$300 \times 10^3$
total environment steps	$1 \times 10^6$
<i>CCGE only</i>	
confidence scale ( $\lambda_{\text{conf}}$ )	200
supervision scaling constant ( $\lambda_{\text{sup}}$ )	1
<i>Oracle 1 (SAC)</i>	
number of hidden layers (all networks)	2
number of neurons per layer (all networks)	64
replay buffer size	$100 \times 10^3$
total environment steps	$100 \times 10^3$
<i>Oracle 1 (SAC)</i>	
number of hidden layers (all networks)	2
number of neurons per layer (all networks)	64
replay buffer size	$100 \times 10^3$
total environment steps	$500 \times 10^3$

### E.4 CCGE and SAC Hyperparameters for Domain Randomized CarRacing

All networks consist of a Convolutional Neural Network (CNN) backbone with an additional Multilayer Perceptron (MLP) at the end. The  $Q$ -value networks have the architecture shown in Fig. 12. The actors have a similar architecture, but omit the single layer MLP and the sum operation.

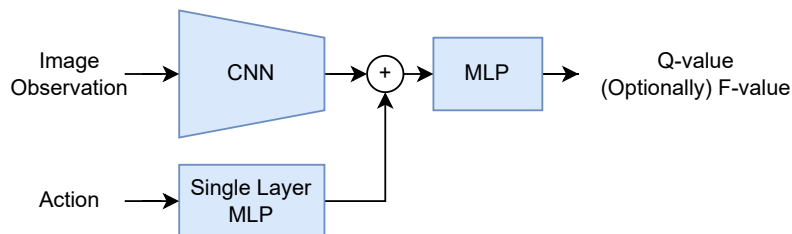


Figure 12: Architecture of the  $Q$ -value network used in the Domain Randomized CarRacing experiments.



Table 4: CCGE and SAC Hyperparameters for Domain Randomized CarRacing.

Parameter	Value
<i>Constants</i>	
<i>Network Architectures</i>	
Convnet backbones	$[3 \times 3 \text{ conv}, 2 \times 2 \text{ maxpool, non-linearity}] \times 4 + [\text{flatten}]$
Convnet number of kernels	$[256, 256, 256, 16]$
<i>Critic MLP head</i>	
number of hidden layers	2
number of neurons per layer	256
<i>Critic single layer MLP</i>	
output size	256
<i>Actor MLP head</i>	
number of hidden layers	1
number of neurons per layer	256
non-linearity	Leaky <i>ReLU</i>
image size	$3 \times 64 \times 64$
starting frame skips	50
framestack	4
optimizer	AdamW (Loshchilov and Hutter 2018; Kingma and Ba 2015)
size of Q ensemble	2
target smoothing coefficient ( $\tau$ )	0.005
entropy coefficient ( $\alpha$ )	auto
target entropy	$-\dim(\mathbf{A})$
train frequency	episodic
number of evaluation episodes	50
evaluation frequency	every $5 \times 10^3$ steps
total environment steps	$150 \times 10^3$
<i>Sweep Hyperparameter Ranges</i>	
minibatch size	$\{50, 100, 150\}$
learning rate	$[0.00001, 0.001]$
discount factor	$[0.90, 0.99]$
replay buffer size	$[20 \times 10^3, 50 \times 10^3]$
<i>CCGE only</i>	
confidence scale ( $\lambda_{\text{conf}}$ )	$[1, 100]$
supervision scaling constant ( $\lambda_{\text{sup}}$ )	$[1.0, 10.0]$
<i>Best Hyperparameters</i>	
minibatch size	150
learning rate	0.00002
discount factor	0.95
replay buffer size	$50 \times 10^3$
<i>CCGE only</i>	
confidence scale ( $\lambda_{\text{conf}}$ )	1
supervision scaling constant ( $\lambda_{\text{sup}}$ )	10.0

## References

- Agarwal, R.; Schwarz, M.; Castro, P. S.; Courville, A. C.; and Bellemare, M. 2021. Deep reinforcement learning at the edge of the statistical precipice. *Advances in Neural Information Processing Systems*, 34.
- Amini, A.; Schwarting, W.; Soleimany, A.; and Rus, D. 2020. Deep Evidential Regression. In Larochelle, H.; Ranzato, M.; Hadsell, R.; Balcan, M. F.; and Lin, H., eds., *Advances in Neural Information Processing Systems*, volume 33, 14927–14937. Curran Associates, Inc.
- Auer, P. 2002. Using confidence bounds for exploitation-exploration trade-offs. *Journal of Machine Learning Research*, 3(Nov): 397–422.
- Bain, M.; and Sammut, C. 1995. A Framework for Behavioural Cloning. In *Machine Intelligence 15*, 103–129.
- Bengio, Y.; Louradour, J.; Collobert, R.; and Weston, J. 2009. Curriculum learning. In *Proceedings of the 26th annual international conference on machine learning*, 41–48.
- Boularias, A.; Kober, J.; and Peters, J. 2011. Relative entropy inverse reinforcement learning. In *Proceedings of the Fourteenth International Conference on Artificial Intelligence and Statistics*, 182–189. JMLR Workshop and Conference Proceedings.
- Brockman, G.; Cheung, V.; Pettersson, L.; Schneider, J.; Schulman, J.; Tang, J.; and Zaremba, W. 2016. Openai gym. *arXiv preprint arXiv:1606.01540*.
- Chen, C.; Wu, Y.-F.; Yoon, J.; and Ahn, S. 2022. TransDreamer: Reinforcement Learning with Transformer World Models. *arXiv preprint arXiv:2202.09481*.
- Chowdhary, G.; Liu, M.; Grande, R.; Walsh, T.; How, J.; and Carin, L. 2014. Off-policy reinforcement learning with Gaussian processes. *IEEE/CAA Journal of Automatica Sinica*, 1(3): 227–238.
- Clements, W. R.; Van Delft, B.; Robaglia, B.-M.; Slaoui, R. B.; and Toth, S. 2019. Estimating risk and uncertainty in deep reinforcement learning. *arXiv preprint arXiv:1905.09638*.
- D’Eramo, C.; Cini, A.; Nuara, A.; Pirotta, M.; Alippi, C.; Peters, J.; and Restelli, M. 2021. Gaussian Approximation for Bias Reduction in Q-Learning. *Journal of Machine Learning Research*, 22(277): 1–51.
- Dhariwal, P.; Hesse, C.; Klimov, O.; Nichol, A.; Plappert, M.; Radford, A.; Schulman, J.; Sidor, S.; Wu, Y.; and Zhokhov, P. 2017. Openai baselines.
- Ellenberger, B. 2018–2019. PyBullet Gymperium.
- Eysenbach, B.; Kumar, A.; and Gupta, A. 2020. Reinforcement learning is supervised learning on optimized data.
- Festor, P.; Luise, G.; Komorowski, M.; and Faisal, A. A. 2021. Enabling risk-aware Reinforcement Learning for medical interventions through uncertainty decomposition. *arXiv preprint arXiv:2109.07827*.
- Gal, Y.; and Ghahramani, Z. 2016. Dropout as a bayesian approximation: Representing model uncertainty in deep learning. In *international conference on machine learning*, 1050–1059. PMLR.
- Haarnoja, T.; Zhou, A.; Abbeel, P.; and Levine, S. 2018a. Soft actor-critic: Off-policy maximum entropy deep reinforcement learning with a stochastic actor. In *International conference on machine learning*, 1861–1870. PMLR.
- Haarnoja, T.; Zhou, A.; Hartikainen, K.; Tucker, G.; Ha, S.; Tan, J.; Kumar, V.; Zhu, H.; Gupta, A.; Abbeel, P.; et al. 2018b. Soft actor-critic algorithms and applications. *arXiv preprint arXiv:1812.05905*.
- Hafner, D.; Lillicrap, T.; Ba, J.; and Norouzi, M. 2019. Dream to control: Learning behaviors by latent imagination. *arXiv preprint arXiv:1912.01603*.
- Hafner, D.; Lillicrap, T.; Norouzi, M.; and Ba, J. 2020. Mastering atari with discrete world models. *arXiv preprint arXiv:2010.02193*.
- Hester, T.; Vecerik, M.; Pietquin, O.; Lanctot, M.; Schaul, T.; Piot, B.; Horgan, D.; Quan, J.; Sendonaris, A.; Osband, I.; et al. 2018. Deep q-learning from demonstrations. In *Proceedings of the AAAI Conference on Artificial Intelligence*, volume 32.
- Ho, J.; Gupta, J.; and Ermon, S. 2016. Model-free imitation learning with policy optimization. In *International Conference on Machine Learning*, 2760–2769. PMLR.
- Jain, M.; Lahlou, S.; Nekoei, H.; Butoi, V.; Bertin, P.; Rector-Brooks, J.; Korablyov, M.; and Bengio, Y. 2021. Deup: Direct epistemic uncertainty prediction. *arXiv preprint arXiv:2102.08501*.
- Kingma, D. P.; and Ba, J. 2015. Adam: A Method for Stochastic Optimization. In *ICLR (Poster)*.
- Kober, J.; and Peters, J. 2010. Imitation and reinforcement learning. *IEEE Robotics & Automation Magazine*, 17(2): 55–62.
- Kumar, A.; Zhou, A.; Tucker, G.; and Levine, S. 2020. Conservative q-learning for offline reinforcement learning. *Advances in Neural Information Processing Systems*, 33: 1179–1191.
- Lakshminarayanan, B.; Pritzel, A.; and Blundell, C. 2017. Simple and scalable predictive uncertainty estimation using deep ensembles. *Advances in neural information processing systems*, 30.
- Lillicrap, T. P.; Hunt, J. J.; Pritzel, A.; Heess, N.; Erez, T.; Tassa, Y.; Silver, D.; and Wierstra, D. 2016. Continuous control with deep reinforcement learning. In *ICLR (Poster)*.
- Liu, Y.; Gupta, A.; Abbeel, P.; and Levine, S. 2018. Imitation from observation: Learning to imitate behaviors from raw video via context translation. In *2018 IEEE International Conference on Robotics and Automation (ICRA)*, 1118–1125. IEEE.
- Loshchilov, I.; and Hutter, F. 2018. Decoupled Weight Decay Regularization. In *International Conference on Learning Representations*.
- Matthies, H. G. 2007. Quantifying uncertainty: modern computational representation of probability and applications. In *Extreme man-made and natural hazards in dynamics of structures*, 105–135. Springer.

- Mnih, V.; Kavukcuoglu, K.; Silver, D.; Rusu, A. A.; Veness, J.; Bellemare, M. G.; Graves, A.; Riedmiller, M.; Fidjeland, A. K.; Ostrovski, G.; et al. 2015. Human-level control through deep reinforcement learning. *nature*, 518(7540): 529–533.
- Moerland, T.; Broekens, J.; and Jonker, C. 2017. Efficient exploration with Double Uncertain Value Networks. In *NIPS 2017: Thirty-first Conference on Neural Information Processing Systems*, 1–17.
- Nair, A.; Dalal, M.; Gupta, A.; and Levine, S. 2020. Accelerating online reinforcement learning with offline datasets. *arXiv preprint arXiv:2006.09359*.
- Nair, A.; McGrew, B.; Andrychowicz, M.; Zaremba, W.; and Abbeel, P. 2018. Overcoming exploration in reinforcement learning with demonstrations. In *2018 IEEE international conference on robotics and automation (ICRA)*, 6292–6299. IEEE.
- Ng, A. Y.; Russell, S. J.; et al. 2000. Algorithms for inverse reinforcement learning. In *Icml*, volume 1, 2.
- Nikolov, N.; Kirschner, J.; Berkenkamp, F.; and Krause, A. 2018. Information-Directed Exploration for Deep Reinforcement Learning. In *International Conference on Learning Representations*.
- Osband, I. 2016. Risk versus uncertainty in deep learning: Bayes, bootstrap and the dangers of dropout. In *NIPS workshop on bayesian deep learning*, volume 192.
- Peng, X. B.; Kumar, A.; Zhang, G.; and Levine, S. 2019. Advantage-weighted regression: Simple and scalable off-policy reinforcement learning. *arXiv preprint arXiv:1910.00177*.
- Raffin, A.; Hill, A.; Ernestus, M.; Gleave, A.; Kanervisto, A.; and Dormann, N. 2019. Stable baselines3.
- Raffin, A.; Kober, J.; and Stulp, F. 2022. Smooth exploration for robotic reinforcement learning. In *Conference on Robot Learning*, 1634–1644. PMLR.
- Rajeswaran, A.; Kumar, V.; Gupta, A.; Vezhani, G.; Schulman, J.; Todorov, E.; and Levine, S. 2018. Learning Complex Dexterous Manipulation with Deep Reinforcement Learning and Demonstrations. In *Proceedings of Robotics: Science and Systems (RSS)*.
- Rezende, D.; and Mohamed, S. 2015. Variational inference with normalizing flows. In *International conference on machine learning*, 1530–1538. PMLR.
- Rosenstein, M. T.; Barto, A. G.; Si, J.; Barto, A.; Powell, W.; and Wunsch, D. 2004. Supervised actor-critic reinforcement learning. *Learning and Approximate Dynamic Programming: Scaling Up to the Real World*, 359–380.
- Rudner, T. G.; Lu, C.; Osborne, M.; Gal, Y.; and Teh, Y. 2021. On pathologies in KL-regularized reinforcement learning from expert demonstrations. *Advances in Neural Information Processing Systems*, 34.
- Schrittwieser, J.; Antonoglou, I.; Hubert, T.; Simonyan, K.; Sifre, L.; Schmitt, S.; Guez, A.; Lockhart, E.; Hassabis, D.; Graepel, T.; et al. 2020. Mastering atari, go, chess and shogi by planning with a learned model. *Nature*, 588(7839): 604–609.
- Schulman, J.; Wolski, F.; Dhariwal, P.; Radford, A.; and Klimov, O. 2017. Proximal Policy Optimization Algorithms. *CoRR*, abs/1707.06347.
- Siegel, N.; Springenberg, J. T.; Berkenkamp, F.; Abdolmaleki, A.; Neunert, M.; Lampe, T.; Hafner, R.; Heess, N.; and Riedmiller, M. 2019. Keep Doing What Worked: Behavior Modelling Priors for Offline Reinforcement Learning. In *International Conference on Learning Representations*.
- Silver, D.; Huang, A.; Maddison, C. J.; Guez, A.; Sifre, L.; Van Den Driessche, G.; Schrittwieser, J.; Antonoglou, I.; Panneershelvam, V.; Lanctot, M.; et al. 2016. Mastering the game of Go with deep neural networks and tree search. *nature*, 529(7587): 484–489.
- Silver, D.; Lever, G.; Heess, N.; Degris, T.; Wierstra, D.; and Riedmiller, M. 2014. Deterministic policy gradient algorithms. In *International conference on machine learning*, 387–395. PMLR.
- Sonabend, A.; Lu, J.; Celi, L. A.; Cai, T.; and Szolovits, P. 2020. Expert-supervised reinforcement learning for offline policy learning and evaluation. *Advances in Neural Information Processing Systems*, 33: 18967–18977.
- Sutton, R. S.; and Barto, A. G. 2018. *Reinforcement learning: An introduction*. MIT press.
- Uchendu, I.; Xiao, T.; Lu, Y.; Zhu, B.; Yan, M.; Simon, J.; Bennice, M.; Fu, C.; Ma, C.; Jiao, J.; et al. 2022. Jump-Start Reinforcement Learning. *arXiv preprint arXiv:2204.02372*.
- Van Hasselt, H.; Guez, A.; and Silver, D. 2016. Deep reinforcement learning with double q-learning. In *Proceedings of the AAAI conference on artificial intelligence*, volume 30.
- Wu, Y.; Tucker, G.; and Nachum, O. 2019. Behavior regularized offline reinforcement learning. *arXiv preprint arXiv:1911.11361*.
- Zhang, X.; and Ma, H. 2018. Pretraining deep actor-critic reinforcement learning algorithms with expert demonstrations. *arXiv preprint arXiv:1801.10459*.
- Zhang, Z.; Pan, Z.; and Kochenderfer, M. J. 2017. Weighted Double Q-learning. In *IJCAI*, 3455–3461.